

# Synthesis, characterization, crystal structure, theoretical studies, and antibacterial activities of P-coordinated mercury(II) complexes containing phosphine–phosphonium salts



Sepideh Samiee<sup>a,\*</sup>, Nadieh Kooti<sup>a</sup>, Hossein Motamedi<sup>b</sup>, Robert W. Gable<sup>c</sup>, Fateme Akhlaghi Bagherjeri<sup>c</sup>

<sup>a</sup> Department of Chemistry, Faculty of Science, Shahid Chamran University, Ahvaz, Iran

<sup>b</sup> Department of Biology, College of Sciences, Shahid Chamran University, Ahvaz, Iran

<sup>c</sup> School of Chemistry, University of Melbourne, Victoria 3010, Australia

## ARTICLE INFO

### Article history:

Received 31 March 2015

Accepted 12 June 2015

Available online 19 June 2015

### Keyword:

Phosphine–phosphonium salt

Mercury(II) complex

Theoretical study

Antibacterial activity

Zwitterionic complex

## ABSTRACT

The reaction of mercury(II) halides with the phosphine–phosphonium salts  $[\text{PPh}_2(\text{CH}_2)_2\text{PPh}_2\text{CH}_2\text{C}(\text{O})\text{C}_6\text{H}_4\text{R}]\text{Br}$  ( $\text{R} = \text{Br}$  (**S**<sup>1</sup>),  $\text{NO}_2$  (**S**<sup>2</sup>)) in methanol affords the zwitterionic mercury(II) complexes  $\{\text{HgX}_2\text{Br}(\text{PPh}_2(\text{CH}_2)_2\text{PPh}_2\text{CH}_2\text{C}(\text{O})\text{C}_6\text{H}_4\text{R})\}$  [ $\text{R} = \text{Br}$ :  $\text{X} = \text{Cl}$  (**1**),  $\text{Br}$  (**2**),  $\text{I}$  (**3**);  $\text{R} = \text{NO}_2$ :  $\text{X} = \text{Cl}$  (**4**),  $\text{Br}$  (**5**),  $\text{I}$  (**6**)]. These complexes were fully characterized by elemental analysis and spectroscopic techniques such as IR, <sup>1</sup>H, <sup>31</sup>P, and <sup>13</sup>C NMR. The structure of complex **4** has been characterized crystallographically. Single crystal X-ray analysis reveals the presence of mononuclear P-coordinated complex containing Hg(II) in a distorted tetrahedral environment. Theoretical studies using density functional theory have been performed on the free ligands (**S**<sup>1</sup> and **S**<sup>2</sup>) and their corresponding complexes (**1**–**6**). Electronic and structural properties of latter compounds were examined and general trends were derived. The natural bonding orbital calculations have also been carried out to understand the nature of the Hg–P bond. The results show that the interactions between the metal atom and phosphorus atom of phosphine group are mainly an electrostatic interaction. In addition, there is a decrease in the charge distribution on the ligand reflecting electron transfer from the ligand to the metal and halogens atoms. The *in vitro* antibacterial activities of the entitled compounds were evaluated against Gram-negative as *Escherichia coli* and *Pseudomonas aeruginosa* bacteria and Gram-positive as *Bacillus subtilis* and *Staphylococcus aureus* and compared with the standard antibacterial drugs.

© 2015 Elsevier Ltd. All rights reserved.

## 1. Introduction

Zwitterionic metal complexes have wide applications in the catalysis and biochemistry due to their heightened solubility in low-polarity media, increased tolerance to polar coordinating solvents, and the avoidance of counteranion effects [1–5]. On the other hand, phosphonium salts have been extensively studied both as valuable intermediates in organic synthesis and as interesting ligands in coordination chemistry [6–13]. It is also well established that in comparison of sulfonium, pyridinium and ammonium salts, phosphonium counter parts offer a great variety of reactivities because of their d-orbital participation [14,15]. Moreover, these types of compounds can be employed as thermally latent initiators or photoinitiators in cationic polymerization [16–18]. The phosphonium salts are most often converted to phosphorus ylides by releasing a proton. The efficiency of metalated phosphorus ylides

in synthetic chemistry has been well documented [19–27]. Most of the interest in the coordination properties of resonance stabilized phosphorus ylides stemming from their bond versatility is due to the presence of different functional groups in their molecular structure [20]. Therefore, phosphorus ylides are known to demonstrate rich coordination chemistry.

In 2009, Ebrahim and co-workers reported the reactivity of the hybrid phosphine–phosphonium salt,  $[\text{PPh}_2\text{CH}_2\text{PPh}_2\text{CH}_2\text{COPh}]\text{Br}$ , with mercury(II) halides [8]. Recently, Sabounchei et al. also reported the synthesis of several zwitterionic complexes of mercury(II) derived from  $\text{PPh}_2\text{CH}_2\text{PPh}_2$  (dppm) and determining the formation constants of entitled complexes in dimethylsulfoxide [9]. In the context of this paper, we report the reactivity of phosphine–phosphonium salts derived from bis(diphenylphosphino)ethane (dppe) towards mercury(II) halides, along with an *in vitro* determination of their antibacterial activity. The X-ray crystal structure of complex **4** demonstrates P-coordination of the ligand to metal atom. In continuous, theoretical studies on entitled phosphonium salts and their corresponding complexes were

\* Corresponding author. Tel.: +98 6113331042; fax: +98 6113337009.

E-mail addresses: [s.samiee@scu.ac.ir](mailto:s.samiee@scu.ac.ir), [samiee.sepideh@gmail.com](mailto:samiee.sepideh@gmail.com) (S. Samiee).

performed by density functional theory (DFT), providing further understanding of the chemical behavior of phosphonium salts and their mercury(II) complexes.

## 2. Experimental

### 2.1. Materials and measurements

All reactions were carried out under dry nitrogen atmospheres using standard Schlenk tube techniques. Solvents were dried and distilled using standard methods [28]. Starting materials were purchased from commercial sources and used without further purification. The phosphine–phosphonium salts, namely  $[\text{PPh}_2(\text{CH}_2)_2\text{PPh}_2\text{CH}_2\text{C}(\text{O})\text{C}_6\text{H}_4\text{Br}]\text{Br}$  (**S**<sup>1</sup>) [29] and  $[\text{PPh}_2(\text{CH}_2)_2\text{PPh}_2\text{CH}_2\text{C}(\text{O})\text{C}_6\text{H}_4\text{NO}_2]\text{Br}$  (**S**<sup>2</sup>), were prepared by following the methods described in the literature [30]. Infrared spectra were collected on samples as KBr pellets using a FT BOMEM MB102 spectrophotometer from 400 to 4000  $\text{cm}^{-1}$ . <sup>31</sup>P, <sup>1</sup>H and <sup>13</sup>C NMR spectra were recorded on 300 MHz Bruker spectrometer in DMSO-*d*<sub>6</sub> as solvent at room temperature. Chemical shifts (ppm) are reported according to internal TMS and external 85% phosphoric acid. Coupling constants are given in Hz. Elemental analyses were performed using a Perkin-Elmer 2400 series analyzer. Melting points were measured on a SMP3 apparatus.

### 2.2. X-ray crystal structure determination

Suitable single crystal of  $[\text{HgCl}_2\text{Br}(\text{PPh}_2(\text{CH}_2)_2\text{PPh}_2\text{CH}_2\text{C}(\text{O})\text{C}_6\text{H}_4\text{NO}_2)]$  (**4**) was grown by slow evaporation of dichloromethane/*n*-hexane solutions. All measurements were performed on an Agilent Technologies SuperNova diffractometer using mirror mono-chromated Cu K $\alpha$  radiation ( $\lambda = 1.54184 \text{ \AA}$ ) at 130 K. Structure solution and refinement were carried out using SHELXS-97 and SHELXL-97, respectively [31,32]. The structure was solved by direct methods and refined by full matrix least-squares methods on  $F^2$  and difference Fourier maps using  $P2_12_12_1$  space group with  $Z = 4$ . All non-hydrogen atoms were refined anisotropically using reflections  $I > 2\sigma(I)$ . Hydrogen atoms were located in ideal positions.

### 2.3. Computational method

The geometries of two ligands and their complexes were fully optimized using DFT with Becke's three-parameter exchange potential and the Lee–Yang–Parr correlation functional (B3LYP) [33] along with the CEP-121G basis set [34]. This basis sets includes effective core potentials (ECP) for mercury, phosphorus and halide (Cl, Br and I) atoms. A starting *ab initio* calculations for **S**<sup>1</sup> and **S**<sup>2</sup> was obtained using the HYPERCHEM 5.02 program [35]. The observed geometry of complex **4** was used as a basis of DFT calculations for investigated complexes. To evaluate and ensure the optimized structures of the molecules, frequency calculations were performed using analytical second derivatives. Beside, the natural bonding orbital (NBO) calculations [36] were performed using the NBO 3.1 program as implemented at the same level of theory. All calculations were carried out using the GAUSSIAN 03 computational chemistry program [37].

### 2.4. Antibacterial tests

The *in vitro* antibacterial activity of phosphonium salts as free ligands (**S**<sup>1</sup> and **S**<sup>2</sup>) and their corresponding mercury(II) complexes (**1–6**) was evaluated by disc diffusion method against two Gram-positive bacteria, namely *Bacillus cereus* (ATCC 6633) and *Staphylococcus aureus* (ATCC 6538), and two Gram-negative bacteria, namely *Escherichia coli* (ATCC 25922) and *Pseudomonas*

*aeruginosa* (ATCC 9027). Penicillin (10  $\mu\text{g}/\text{disk}$ ) and Gentamicin (10  $\mu\text{g}/\text{disk}$ ) were used as standard antibacterial drugs. All compounds were dissolved in dimethylsulfoxide (DMSO) at 5, 10, 20 and 40 mg/mL concentration. Then sterile blank discs (6.4 mm) were saturated with these concentrations, so the effective dose per disc of prepared compounds were as 0.2, 0.4, 0.8 and 1 mg. Bacterial cultures were adjusted to 0.5 McFarland turbidity and lawn culture was then prepared on nutrient agar (Merck, Germany) plates. The prepared discs were placed on bacterial culture. Simultaneously, discs saturated with DMSO were used as above as negative control. Standard antibiotic discs were also tested against these bacteria as control. The cultures were incubated at 37 °C for 24 h. The zone of inhibition was calculated in millimeters.

### 2.5. Synthesis of compounds

#### 2.5.1. $[\text{PPh}_2(\text{CH}_2)_2\text{PPh}_2\text{CH}_2\text{C}(\text{O})\text{C}_6\text{H}_4\text{Br}]\text{Br}$ (**S**<sup>1</sup>)

The ligand was prepared by the reaction of bis(diphenylphosphino)ethane (dppe) (0.398 g, 1 mmol) with 2,4-dibromoacetophenone (0.291 g, 1.05 mmol) in dry acetone at room temperature overnight. The resulting solution was filtered off, and the precipitate washed with diethyl ether and dried under vacuum [29]. Yield: 0.59 g, 86%. M.p. 145–147 °C. *Anal. Calc.* for  $\text{C}_{34}\text{H}_{30}\text{Br}_2\text{OP}_2$ : C, 60.38; H, 4.47. Found: C, 60.83; H, 4.75%. Selected IR absorption in KBr ( $\text{cm}^{-1}$ ): 1672 ( $\nu_{\text{C=O}}$ ). <sup>1</sup>H NMR ( $\text{CDCl}_3$ ):  $\delta_{\text{H}} = 2.23$  (m, 2H, CH<sub>2</sub>); 3.14 (m, 2H, CH<sub>2</sub>); 5.99 (d, 2H, PCH<sub>2</sub>CO, <sup>2</sup> $J_{\text{PH}} = 12.99$ ); 7.28–8.16 (m, 24H, Ph). <sup>31</sup>P{<sup>1</sup>H} NMR ( $\text{CDCl}_3$ ):  $\delta_{\text{P}} = -14.89$  (br, PPh<sub>2</sub>); 23.65 (d, PCH<sub>2</sub>CO, <sup>3</sup> $J_{\text{PP}} = 44.27$ ). <sup>13</sup>C{<sup>1</sup>H} NMR ( $\text{CDCl}_3$ ):  $\delta_{\text{C}} = 19.84$  (br, CH<sub>2</sub>); 35.75 (d, PCH<sub>2</sub>CO, <sup>1</sup> $J_{\text{PC}} = 58.56$ ); 117.07–135.34 (Ph); 191.59 (s, CO).

#### 2.5.2. $[\text{PPh}_2(\text{CH}_2)_2\text{PPh}_2\text{CH}_2\text{C}(\text{O})\text{C}_6\text{H}_4\text{NO}_2]\text{Br}$ (**S**<sup>2</sup>)

The title ligand was prepared by a similar procedure to that of ligand (**S**<sup>1</sup>) using dppe and 2-bromo-4'-nitroacetophenone (0.256 g, 1.05 mmol), as reported previously [30]. Yield: 0.53 g, 82%. M.p. 172–173 °C (Reported: 169–171 °C). IR (KBr,  $\text{cm}^{-1}$ ): 1683 ( $\nu_{\text{C=O}}$ ). <sup>1</sup>H NMR ( $\text{CDCl}_3$ ):  $\delta_{\text{H}} = 2.24$  (m, 2H, CH<sub>2</sub>); 3.24 (m, 2H, CH<sub>2</sub>); 6.26 (d, 2H, PCH<sub>2</sub>CO, <sup>2</sup> $J_{\text{PH}} = 12.27$ ); 7.27–8.42 (m, 24H, Ph). <sup>31</sup>P{<sup>1</sup>H} NMR ( $\text{CDCl}_3$ ):  $\delta_{\text{P}} = -15.05$  (br, PPh<sub>2</sub>); 20.93 (d, PCH<sub>2</sub>CO, <sup>3</sup> $J_{\text{PP}} = 43.18$ ). <sup>13</sup>C{<sup>1</sup>H} NMR ( $\text{CDCl}_3$ ):  $\delta_{\text{C}} = 19.20$  (br, CH<sub>2</sub>); 36.43 (d, PCH<sub>2</sub>CO, <sup>1</sup> $J_{\text{PC}} = 58.48$ ); 116.80–150.78 (Ph); 191.52 (d, CO, <sup>2</sup> $J_{\text{PC}} = 6.04$ ).

#### 2.5.3. $[\text{HgCl}_2\text{Br}(\text{PPh}_2(\text{CH}_2)_2\text{PPh}_2\text{CH}_2\text{C}(\text{O})\text{C}_6\text{H}_4\text{Br})]$ (**1**)

To a solution of HgCl<sub>2</sub> (0.098 g, 0.36 mmol) in methanol (8 mL) under nitrogen, was added a methanolic solution of **S**<sup>1</sup> (0.202 g, 0.36 mmol). The resultant mixture was stirred at room temperature for 3 h. The white precipitate was isolated, washed twice with 15 ml methanol and dried *in vacuo*. Yield: 0.34 g, 71%. M.p. 153–155 °C. *Anal. Calc.* for  $\text{C}_{34}\text{H}_{30}\text{Br}_2\text{Cl}_2\text{HgOP}_2$ : C, 43.08; H, 3.19. Found: C, 42.86; H, 3.07%. IR (KBr,  $\text{cm}^{-1}$ ): 1676 ( $\nu_{\text{C=O}}$ ). <sup>1</sup>H NMR (DMSO-*d*<sub>6</sub>):  $\delta_{\text{H}} = 3.007$  (br, 2H, CH<sub>2</sub>); 3.63 (br, 2H, CH<sub>2</sub>); 5.78 (d, 2H, PCH<sub>2</sub>CO, <sup>2</sup> $J_{\text{PH}} = 12.50$ ); 7.51–8.02 (m, 24H, Ph). <sup>31</sup>P{<sup>1</sup>H} NMR (DMSO-*d*<sub>6</sub>):  $\delta_{\text{P}} = 14.39$  (d, PPh<sub>2</sub>, <sup>3</sup> $J_{\text{PP}} = 63.78$ ); 22.48 (d, PCH<sub>2</sub>CO, <sup>3</sup> $J_{\text{PP}} = 62.20$ ). <sup>13</sup>C{<sup>1</sup>H} NMR (DMSO-*d*<sub>6</sub>):  $\delta_{\text{C}} = 18.08$  (br, CH<sub>2</sub>); 28.80 (m, PCH<sub>2</sub>CO); 117.86–135.26 (Ph); 192.14 (s, CO).

#### 2.5.4. $[\text{HgBr}_3(\text{PPh}_2(\text{CH}_2)_2\text{PPh}_2\text{CH}_2\text{C}(\text{O})\text{C}_6\text{H}_4\text{Br})]$ (**2**)

This complex was prepared in the same way as for **1** using mercury(II) bromide (0.13 g, 0.36 mmol). Yield: 0.40 g, 78%. M.p. 201–203 °C. *Anal. Calc.* for  $\text{C}_{34}\text{H}_{30}\text{Br}_4\text{HgOP}_2$ : C, 39.39; H, 2.92. Found: C, 39.52; H, 2.99%. IR (KBr,  $\text{cm}^{-1}$ ): 1676 ( $\nu_{\text{C=O}}$ ). <sup>1</sup>H NMR (DMSO-*d*<sub>6</sub>):  $\delta_{\text{H}} = 2.97$  (br, 2H, CH<sub>2</sub>); 3.60 (m, 2H, CH<sub>2</sub>); 5.79 (d, 2H, PCH<sub>2</sub>CO, <sup>2</sup> $J_{\text{PH}} = 12.52$ ); 7.52–8.01 (m, 24H, Ph). <sup>31</sup>P{<sup>1</sup>H} NMR (DMSO-*d*<sub>6</sub>):  $\delta_{\text{P}} = 17.95$  (br, PPh<sub>2</sub>); 26.23 (d, PCH<sub>2</sub>CO, <sup>3</sup> $J_{\text{PP}} = 55.96$ ).

$^{13}\text{C}\{^1\text{H}\}$  NMR (DMSO- $d_6$ ):  $\delta_{\text{C}} = 18.44$  (br,  $\text{CH}_2$ ); 117.91–135.47 (Ph); 192.23 (s, CO); ( $\text{CH}_2$ , was not seen).

#### 2.5.5. $[\text{HgI}_2\text{Br}(\text{PPh}_2(\text{CH}_2)_2\text{PPh}_2\text{CH}_2\text{C}(\text{O})\text{C}_6\text{H}_4\text{Br})]$ (**3**)

This complex was prepared in the same way as for **1** using mercury(II) iodide (0.16 g, 0.36 mmol). Yield: 0.46 g, 80%. M.p. 220–222 °C. *Anal. Calc.* for  $\text{C}_{34}\text{H}_{30}\text{BrI}_2\text{HgNO}_3\text{P}_2$ : C, 36.11; H, 2.67. Found: C, 35.97; H, 2.83%. IR (KBr,  $\text{cm}^{-1}$ ): 1675 ( $\nu_{\text{C}=\text{O}}$ ).  $^1\text{H}$  NMR (DMSO- $d_6$ ):  $\delta_{\text{H}} = 2.86$  (br, 2H,  $\text{CH}_2$ ); 3.51 (br, 2H,  $\text{CH}_2$ ); 5.78 (d, 2H,  $\text{PCH}_2\text{CO}$ ,  $^2J_{\text{PH}} = 12.50$ ); 7.49–8.01 (m, 24H, Ph).  $^{31}\text{P}\{^1\text{H}\}$  NMR (DMSO- $d_6$ ):  $\delta_{\text{P}} = 3.74$  (br,  $\text{PPh}_2$ ); 22.60 (d,  $\text{PCH}_2\text{CO}$ ,  $^3J_{\text{PP}} = 61.76$ ).  $^{13}\text{C}\{^1\text{H}\}$  NMR (DMSO- $d_6$ ):  $\delta_{\text{C}} = 18.37$  (br,  $\text{CH}_2$ ); 31.69 (m,  $\text{PCH}_2\text{CO}$ ); 117.80–135.32 (Ph); 192.15 (d, CO,  $^1J_{\text{PC}} = 5.91$ ).

The following complexes were made similarly using the appropriate starting ligand **S**<sup>2</sup> and related mercury(II) halides. All reactions were also carried out under an atmosphere of dry nitrogen.

#### 2.5.6. $[\text{HgCl}_2\text{Br}(\text{PPh}_2(\text{CH}_2)_2\text{PPh}_2\text{CH}_2\text{C}(\text{O})\text{C}_6\text{H}_4\text{NO}_2)]$ (**4**)

Yield: 0.33 g, 72%. M.p. >250 °C (decomposes). *Anal. Calc.* for  $\text{C}_{34}\text{H}_{30}\text{BrCl}_2\text{HgNO}_3\text{P}_2$ : C, 43.61; H, 3.76; N, 1.53. Found: C, 43.65; H, 3.32; N, 1.28%. IR (KBr,  $\text{cm}^{-1}$ ): 1684 ( $\nu_{\text{C}=\text{O}}$ ).  $^1\text{H}$  NMR (DMSO- $d_6$ ):  $\delta_{\text{H}} = 3.05$  (br, 2H,  $\text{CH}_2$ ); 3.66 (br, 2H,  $\text{CH}_2$ ); 5.88 (d, 2H,  $\text{PCH}_2\text{CO}$ ,  $^2J_{\text{PH}} = 11.75$ ); 7.56–8.46 (m, 24H, Ph).  $^{31}\text{P}\{^1\text{H}\}$  NMR (DMSO- $d_6$ ):  $\delta_{\text{P}} = 14.68$  (d,  $\text{PPh}_2$ ,  $^3J_{\text{PP}} = 63.01$ ); 22.37 (d,  $\text{PCH}_2\text{CO}$ ,  $^3J_{\text{PP}} = 64.87$ ).  $^{13}\text{C}\{^1\text{H}\}$  NMR (DMSO- $d_6$ ):  $\delta_{\text{C}} = 19.90$  (br,  $\text{CH}_2$ ); 35.77 (d,  $\text{PCH}_2\text{CO}$ ,  $^1J_{\text{PC}} = 58.71$ ); 117.07–141.39 (Ph); 191.28 (s, CO).

#### 2.5.7. $[\text{HgBr}_3(\text{PPh}_2(\text{CH}_2)_2\text{PPh}_2\text{CH}_2\text{C}(\text{O})\text{C}_6\text{H}_4\text{NO}_2)]$ (**5**)

Yield: 0.38 g, 77%. M.p. >138 °C (decomposes). *Anal. Calc.* for  $\text{C}_{34}\text{H}_{30}\text{Br}_3\text{HgNO}_3\text{P}_2$ : C, 40.72; H, 3.02; N, 1.40. Found: C, 40.33; H, 3.11; N, 1.21%. IR (KBr,  $\text{cm}^{-1}$ ): 1686 ( $\nu_{\text{C}=\text{O}}$ ).  $^1\text{H}$  NMR (DMSO- $d_6$ ):  $\delta_{\text{H}} = 3.04$  (br, 2H,  $\text{CH}_2$ ); 3.48 (br, 2H,  $\text{CH}_2$ ); 5.87 (d, 2H,  $\text{PCH}_2\text{CO}$ ,  $^2J_{\text{PH}} = 11.25$ ); 7.53–8.46 (m, 24H, Ph).  $^{31}\text{P}\{^1\text{H}\}$  NMR (DMSO- $d_6$ ):  $\delta_{\text{P}} = 18.28$  (br,  $\text{PPh}_2$ ); 22.36 (d,  $\text{PCH}_2\text{CO}$ ,  $^3J_{\text{PP}} = 63.59$ ).  $^{13}\text{C}\{^1\text{H}\}$  NMR (DMSO- $d_6$ ):  $\delta_{\text{C}} = 21.57$  (br,  $\text{CH}_2$ ); 36.02 (d,  $\text{PCH}_2\text{CO}$ ,  $^1J_{\text{PC}} = 58.18$ ); 117.59–134.65 (Ph); 191.45 (s, CO).

#### 2.5.8. $[\text{HgI}_2\text{Br}(\text{PPh}_2(\text{CH}_2)_2\text{PPh}_2\text{CH}_2\text{C}(\text{O})\text{C}_6\text{H}_4\text{NO}_2)]$ (**6**)

Yield: 0.45 g, 82%. M.p. >225 °C (decomposes). *Anal. Calc.* for  $\text{C}_{34}\text{H}_{30}\text{BrI}_2\text{HgNO}_3\text{P}_2$ : C, 37.23; H, 2.76; N, 1.28. Found: C, 37.24; H, 2.96; N, 1.08%. IR (KBr,  $\text{cm}^{-1}$ ): 1686 ( $\nu_{\text{C}=\text{O}}$ ).  $^1\text{H}$  NMR (DMSO- $d_6$ ):  $\delta_{\text{H}} = 2.73$  (br, 2H,  $\text{CH}_2$ ); 3.08 (br, 2H,  $\text{CH}_2$ ); 5.99 (d, 2H,  $\text{PCH}_2\text{CO}$ ,  $^2J_{\text{PH}} = 12.50$ ); 7.62–8.58 (m, 24H, Ph).  $^{31}\text{P}\{^1\text{H}\}$  NMR (DMSO- $d_6$ ):  $\delta_{\text{P}} = 2.61$  (br,  $\text{PPh}_2$ ); 22.51 (d,  $\text{PCH}_2\text{CO}$ ,  $^3J_{\text{PP}} = 58.01$ ).  $^{13}\text{C}\{^1\text{H}\}$  NMR (DMSO- $d_6$ ):  $\delta_{\text{C}} = 18.21$  (m,  $\text{CH}_2$ ); 33.04 (m,  $\text{PCH}_2\text{CO}$ ); 117.66–151.30 (Ph); 192.12 (s, CO).

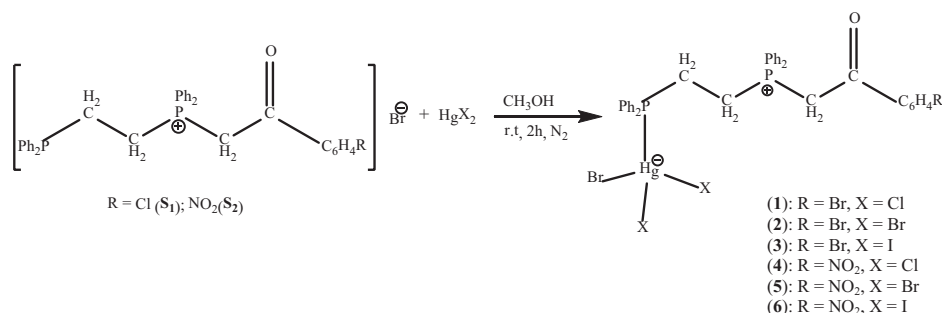
## 3. Results and discussion

### 3.1. Synthesis

The reaction of phosphine–phosphonium salts (**S**<sup>1</sup> and **S**<sup>2</sup>) with mercury(II) halides in 1:1 molar ratio gave the zwitterionic P-coordinated complexes (**1–6**) in good yield. The ligands **S**<sup>1</sup> and **S**<sup>2</sup> were already synthesized way back in 2010 [29,30]. These species are fairly soluble in halogenated solvents such as chloroform and dichloromethane but insoluble in non-polar solvents such as *n*-pentane and *n*-hexane. The reactions studied in the present work are summarized in Scheme 1.

### 3.2. Spectroscopic studies

The selected important IR and NMR data for all complexes and free ligands are presented in Table 1. The  $\nu(\text{CO})$ , which is sensitive to complexation, occurs around  $1680\text{ cm}^{-1}$  in the parent phosphonium salts. The comparison of the carbonyl stretch of complexes (**1–6**) and free ligands show that this absorption band appears near to that of the free ligands and close to those observed in other P-coordinated complexes [8,26]. Coordination of the ylide through carbon causes an increase in  $\nu(\text{CO})$ , while for O-coordination a decrease of  $\nu(\text{CO})$  is expected [22]. Therefore, the Infrared data indicates that the interaction of the free phosphonium salts with mercury(II) halides is only through the  $\text{PPh}_2$  group to metal center.



**Scheme 1.** Synthesis route for preparation of zwitterionic mercury(II) halides complexes.

**Table 1**  
Selected IR and NMR spectral data for phosphonium salts and their metal complexes (**1–6**).

Compound	IR	$^1\text{H}$ NMR	$^{31}\text{P}$ NMR		$^{13}\text{C}$ NMR	Reference
	$\nu(\text{CO})$	$\delta$ $\text{PCH}_2$ ( $^2J_{\text{P-H}}$ )	$\delta$ $\text{PPh}_2$ ( $^2J_{\text{P-P}}$ )	$\delta$ $\text{PCH}_2$ ( $^2J_{\text{P-P}}$ )	$\delta$ CO	
<b>S</b> <sup>1</sup>	1672	5.99(1.99)	−14.89(44.34)	23.65(44.27)	191.59	[29]
<b>1</b>	1676	5.78(12.50)	14.39(63.87)	22.48(62.20)	192.14	This work
<b>2</b>	1676	5.79(12.52)	17.95(br)	26.23(55.96)	192.23	This work
<b>3</b>	1674	5.78(12.59)	3.74(br)	22.60(61.76)	192.15	This work
<b>S</b> <sup>2</sup>	1683	6.26(12.27)	−15.05(br)	20.93(43.18)	191.52	[30]
<b>4</b>	1684	5.88(11.75)	14.68(63.01)	22.37(64.87)	191.28	This work
<b>5</b>	1685	5.87(11.25)	18.28(br)	22.36(63.59)	191.45	This work
<b>6</b>	1686	5.99(12.50)	2.61(br)	22.51(58.01)	192.12	This work

$\nu$  ( $\text{cm}^{-1}$ ),  $\delta$  (ppm),  $J$  (Hz); br, broad.

In the  $^{31}\text{P}\{^1\text{H}\}$  NMR spectra, the signal due to phosphine group appears as a doublet. The significant downfield shift of this signal to that phosphine of the related phosphonium salts is in agreement with the P-bonding of the ligands. In this regard, the chemical shift values of phosphonium group ( $\text{PCH}_2\text{CO}$ ) have either remained unaffected or shifted slightly with reference to those of the parent salts. Moreover, in the  $^1\text{H}$  NMR spectra of complexes (**1–6**), the doublet due to methyl group around 5.80 ppm with a coupling constant  $^2J_{\text{P-H}}$  of 12 Hz, appears in the same region as observed for the free ligands, again in agreement with P-coordination. In the  $^{13}\text{C}\{^1\text{H}\}$  NMR spectra of all six complexes, the signals attributed to the carbonyl group have also remained unaffected due to complexation (see Table 1). Similar behavior have been observed earlier in the case of P-coordinated complexes of mercury(II) halides [8,9]. No  $^{199}\text{Hg}$  satellites were observed in the  $^{31}\text{P}$ ,  $^1\text{H}$  and  $^{13}\text{C}$  NMR spectra, which means that the Hg–P bond probably are breaking and forming quickly, as previously reported in the ylide complexes of Hg(II) [23] and Ag(I) [21]. Hence, the results of spectroscopic studies clearly demonstrate that the monodentate coordination of the phosphine–phosphonium salts towards the mercury center through the phosphorus atom of phosphine group.

### 3.3. Crystal structure analysis

The X-ray crystal structure of  $[\text{HgCl}_2(\text{Br})(\text{PPh}_2(\text{CH}_2)_2\text{PPh}_2\text{CH}_2\text{C}(\text{O})\text{C}_6\text{H}_4\text{NO}_2)]$  (**4**) are shown in Fig. 1. Relevant parameters concerning data collection and refinement are given in Table 2 and selected bond distances and angles are listed in Table 3. Fractional atomic coordinates and equivalent isotropic displacement coefficients ( $U_{\text{eq}}$ ) for the non-hydrogen atoms of the complex is available as Supplementary material.

The X-ray analysis reveals the P-coordination mode of ligand **S**<sup>2</sup> to metal center in complex **4**. The mercury is surrounded by one phosphorus atom and three halide ligands in a distorted tetrahedral geometry ( $95.8(8)$ – $120.16(11)^\circ$ ). As can be seen in Fig. 1, the  $\text{Br}^-$  ion of **S**<sup>2</sup> is bonded to metal center, which can be explained by both the preference of Hg(II) for four coordination and the stability of the 18 electron configuration around Hg(II). The Hg–P

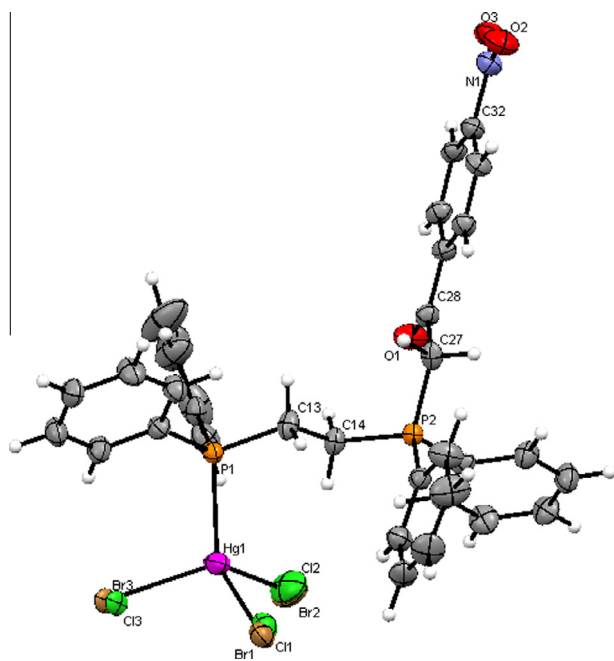


Fig. 1. ORTEP view of the X-ray crystal structure of complex **4**.

Table 2  
Crystal data and experimental details for complex **4**.

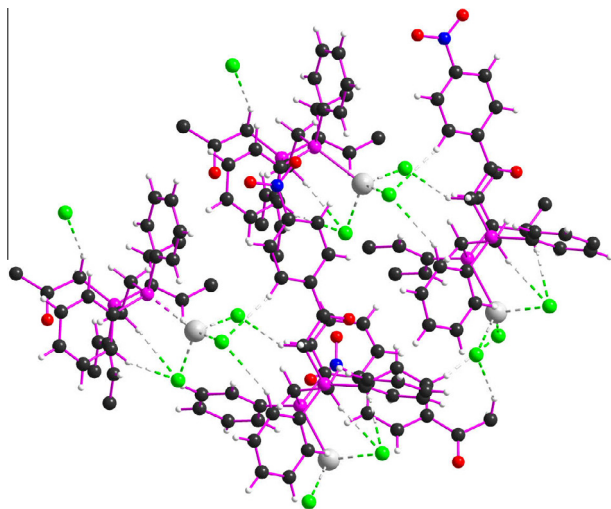
Empirical formula	$\text{C}_{34}\text{H}_{30}\text{NO}_3\text{P}_2\text{Cl}_{1.23}\text{Br}_{1.76}\text{Hg}$
Formula weight	947.94
Temperature (K)	130.01(10)
Wavelength (Å)	1.54184
Crystal system	orthorhombic
Space group	$P2_12_12_1$
<i>a</i> (Å)	9.66483(8)
<i>b</i> (Å)	15.23112(13)
<i>c</i> (Å)	23.75760(18)
Volume (Å <sup>3</sup> )	3497.27(5)
<i>Z</i>	4
$\mu$ (mm <sup>-1</sup> )	12.267
$2\theta$ range for data collection (°)	6.894 to 154.218
Index ranges	$-12 \leq h \leq 9$ $-19 \leq k \leq 19$ $-30 \leq l \leq 25$
Reflections collected	38589
Independent reflections	7358 [ $R_{\text{int}} = 0.0395$ ]
Data/restraints/parameters	7358/9/413
Goodness-of-fit on $F^2$	1.060
Final <i>R</i> indices [ $I > 2\sigma(I)$ ]	$R_1 = 0.0368$ , $wR_2 = 0.0893$
<i>R</i> indices (all data)	$R_1 = 0.0376$ , $wR_2 = 0.0899$

Table 3  
Selected bond lengths (Å) and bond angles (°) for complex **4**.

<i>Bond lengths</i>	
Hg(1)–P(1)	2.460(17)
Hg(1)–Cl(1)	2.399(7)
Hg(1)–Cl(2)	2.401(7)
Hg(1)–Cl(3)	2.399(7)
Hg(1)–Br(1)	2.637(2)
Hg(1)–Br(2)	2.646(2)
Hg(1)–Br(3)	2.640(2)
O(1)–C(28)	1.217(10)
P(1)–C(27)	1.813(8)
C(27)–C(28)	1.515(9)
[P(2) ... O(1)]	2.860
<i>Bond angles</i>	
Cl(1)–Hg(1)–Cl(2)	95.8(8)
Cl(1)–Hg(1)–Cl(3)	107.8(2)
Cl(2)–Hg(1)–Cl(3)	114.0(6)
Br(1)–Hg(1)–Br(2)	101.00(14)
Br(1)–Hg(1)–Br(3)	107.88(9)
Br(2)–Hg(1)–Br(3)	109.0(2)
Cl(1)–Hg(1)–P(1)	118.9(6)
Cl(2)–Hg(1)–P(1)	109.6(8)
Cl(3)–Hg(1)–P(1)	110.2(4)
Br(1)–Hg(1)–P(1)	120.16(11)
Br(2)–Hg(1)–P(1)	110.81(12)
Br(3)–Hg(1)–P(1)	107.6(2)

distance of 2.460(17) Å in this complex is in agreement with the values reported for P-coordinated monomeric complexes [8,30,26].

During the refinement it became apparent that there is substitution disorder in each of the halogen atoms attached to the mercury; the final occupancy factors (Br & Cl) were 0.656(8) & 0.344(8), 0.696(9) & 0.304(9) and 0.413(7) & 0.587(7) giving rise to a 7:5 overall ratio. During the refinement the Hg–Br and Hg–Cl distances were restrained to be equal, while the Br–Cl separation was constrained to be 0.3 Å; the anisotropic displacement parameters of the atoms on each site were also constrained to be equal. The maximum electron density peak was  $2.6 \text{ e}\text{Å}^{-3}$ , which is 1.07 Å far from Hg. As can be seen in molecular structure of this complex, the phosphorus and oxygen atoms are cis oriented due to strong 1,4-P $\cdots$ O intramolecular interactions between the positively charged P atom and the negatively charged O atom, as described previously for phosphorus ylides and their mercury(II) complexes [38] (see Table 3). The nitro group makes a dihedral angle of  $6.5(3)^\circ$  with the aromatic ring, while the orientation of the



**Fig. 2.** Representation of intermolecular contacts of complex **4**. Dashed lines represent short contacts. Color code: Hg grey, P purple, C black, N blue, O red and Cl#Br green (for the occupancy ratios refer to Table 3). (Colour online.)

**Table 4**

Significant non-classical hydrogen bonds (interatomic distance (Å) and bond angles °) found in the structures of complex **4**.

D–H···A	D–H	H···A	D···A	<(DHA)
C2–H2···Br3	0.95	3.05	3.896(13)	149.1
C8–H8···Br2	0.95	2.91	3.827(12)	162.1
C8–H8···Cl2	0.95	2.88	3.77(3)	157.5
C13–H13···Br1 <sup>i</sup>	0.99	2.80	3.762(9)	163.5
C13–H13···Cl1 <sup>i</sup>	0.99	2.90	3.84(2)	160.5
C14–H14···Br2	0.99	2.91	3.874(9)	163.8
C14–H14···Cl2	0.99	2.70	3.67(2)	166.3
C20–H20···Br3 <sup>i</sup>	0.95	2.73	3.578(14)	149.5
C20–H20···Cl3 <sup>i</sup>	0.95	2.72	3.57(2)	148.9
C27–H27···Br1 <sup>i</sup>	0.99	2.70	3.536(8)	142.6
C27–H27···Cl1 <sup>i</sup>	0.99	2.82	3.694(16)	148.3
C14–H14···O1	0.99	2.54	3.132(9)	118.5
C26–H26···O3 <sup>ii</sup>	0.95	2.56	3.437(11)	154.3
C27–H27···O3 <sup>ii</sup>	0.99	2.34	3.299(9)	161.9

i, 2 – X, 1/2 + Y, 3/2 – Z; ii, 1/2 + X, 3/2 – Y, 1 – Z.

nitrobenzoyl group is such that all of the atoms of the benzoyl group are coplanar with the phosphorus atom (the greatest deviation is related to C27 (0.030 Å)). Crystal packing of complex **4** is presented in Fig. 2. There are several intramolecular C–H···Cl and C–H···Br non-classic hydrogen bond interactions, with hydrogen atoms from three phenyl rings and one of the aliphatic carbon

**Table 5**

The Selected Optimized bond lengths (Å) and bond angles (°) for the free ligands (**S**<sup>1</sup>) and (**S**<sup>2</sup>).

Compounds	<b>S</b> <sup>1</sup>	<b>S</b> <sup>2</sup>
<i>Bond lengths</i>		
P(1)–C(13)	1.940	1.940
P(2)–C(14)	1.899	1.899
C(13)–C(14)	1.550	1.550
C(27)–C(28)	1.527	1.524
C(28)–O(1)	1.268	1.266
P(2)···O(1)	3.044	3.056
P(2)···Br	4.201	4.189
<i>Bond angles</i>		
P(1)–C(13)–C(14)	111.49	111.44
P(2)–C(13)–C(14)	114.11	114.06
C(6)–P(1)–C(7)	102.50	102.64
C(15)–P(2)–C(21)	114.68	110.96

atoms which, presumably, influence the conformation of phosphorus ligand. The molecules are linked together via several other intermolecular C–H···Cl, C–H···Br and C–H···O interactions to form a 3D H-bonded network (see Table 4).

### 3.4. Theoretical studies

We were interested i) to obtain the geometric and electronic structures of phosphonium salts as free ligands and ii) to compare the structure, stability, electronic and thermochemical properties of zwitterionic mercury(II) complexes. Therefore we launched our investigation on a number of these types of compounds applying density functional theory (DFT) calculations. To the best of our knowledge, the geometries of phosphonium salts (**S**<sup>1</sup> and **S**<sup>2</sup>) and their metal complexes (**1–6**) were fully optimized at B3LYP/CEP-121G level of theory. However, the theoretical study of phosphine–phosphonium salts derived from bis(diphenylphosphino)ethane and corresponding complexes have not been reported.

#### 3.4.1. Geometry and electronic properties of phosphine–phosphonium salts

The lowest energy of optimized geometries of **S**<sup>1</sup> and **S**<sup>2</sup> as free ligands is shown in Fig. 3. The important optimized geometrical parameters such as bond lengths and angles listed in Table 5 are in accordance with atom numbering scheme given in ORTEP views of compound **4**.

The final optimized structure of these ligands indicates that the bromine ion is located near the phosphorus atom of phosphonium group (≈4 Å). This may suggest that there is an intramolecular

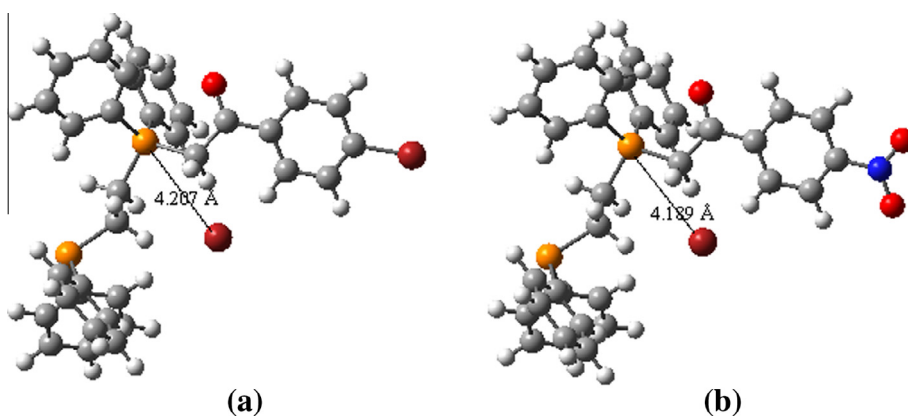


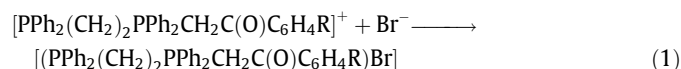
**Fig. 3.** The optimized geometry structures of phosphine–phosphonium salts (a) **S**<sup>1</sup> and (b) **S**<sup>2</sup>.

**Table 6**

HOMO (hartree), LUMO (hartree), gap energy (eV), hardness (eV), NBO charges and Wiberg bond indices of the [(Ph<sub>2</sub>P(CH<sub>2</sub>)<sub>2</sub>PPh<sub>2</sub>CHC(O)C<sub>6</sub>H<sub>4</sub>R)] (R = Br (**S**<sup>1</sup>), NO<sub>2</sub> (**S**<sup>2</sup>)) free ligands.

Compound	<b>S</b> <sup>1</sup>	<b>S</b> <sup>2</sup>
HOMO	-0.196	-0.203
LUMO	-0.090	-0.132
Gap	2.88	1.91
η	1.44	0.95
<i>NBO charges</i>		
P(1)	0.734	0.735
P(2)	1.430	1.431
Br	-0.873	-0.864
O(1)	-0.623	-0.606
C(13)	-0.611	-0.612
C(14)	-0.602	-0.601
C(27)	-0.724	-0.730
C(28)	0.577	0.578
C(32)	-0.046	0.091
Br(1)	0.043	-
N(1)	-	0.447
O(2)	-	-0.359
O(3)	-	-0.368
<i>WBIs</i>		
P(1)-C(13)	0.898	0.897
P(2)-C(14)	0.933	0.942
P(2)-C(27)	0.933	0.931
C(13)-C(14)	1.041	1.041
C(27)-C(28)	1.013	1.019
C(28)-O(1)	1.661	1.682
P(2)-Br	0.005	0.005

interaction between the phosphonium group and the bromine ion. We are interested to figure out, the bromine ion acts only as a counter ion or there is a bonding interaction with phosphonium group in these ligands. To shed some light about this question, the bonding energy was calculated according to the following formation reaction (1):



The results demonstrate that the latter energies in compounds **S**<sup>1</sup> and **S**<sup>2</sup> are -90.73 and -94.65 kcal mol<sup>-1</sup>, respectively. Due to the obtained values for bonding energy, it can be suggested that the bromine ion possesses a bonding interaction to phosphorus

atom of phosphonium group, and the [(PPh<sub>2</sub>(CH<sub>2</sub>)<sub>2</sub>PPh<sub>2</sub>CH<sub>2</sub>C(O)C<sub>6</sub>H<sub>4</sub>R)Br] formulation is more reliable than [PPh<sub>2</sub>(CH<sub>2</sub>)<sub>2</sub>PPh<sub>2</sub>CH<sub>2</sub>C(O)C<sub>6</sub>H<sub>4</sub>R]Br.

Natural bond orbital (NBO) analyses to obtain electronic properties such as the gap energy, partial charge of atoms and Wiberg bond index (WBI) were also investigated (see Table 6). As can be seen in this table, when the R group was changed, the LUMO energy of ligand **S**<sup>2</sup> decreased comparing to ligand **S**<sup>1</sup>. In this regard, the gap energy was found as **S**<sup>1</sup> > **S**<sup>2</sup>, which indicates that the ligand containing nitro is softer than the ligand containing bromine. Hence, the ligand **S**<sup>2</sup>, namely [(PPh<sub>2</sub>(CH<sub>2</sub>)<sub>2</sub>PPh<sub>2</sub>CH<sub>2</sub>C(O)C<sub>6</sub>H<sub>4</sub>NO<sub>2</sub>)Br], can be considered as the more reactive ligand.

Comparing partial atomic charge between **S**<sup>1</sup> and **S**<sup>2</sup>, the partial charge of C(32) is the only difference in these ligands. The considerable variation in the charge distribution of C(32) arises from the electron donation of the Br atom to the phenyl groups via the p orbital into the π orbital of the phenyl group. Furthermore, due to the partial atomic charges on phosphorus atoms and the above results of final optimized geometries of ligands, it can be again concluded that there is an interaction between bromine ion and P(2) atom (see Table 6).

### 3.4.2. Geometry and electronic properties of zwitterionic mercury(II) complexes

According to result of spectroscopic section, it can be assumed that the structure of other synthesized complexes would be similar to complex 4. Table 7 gives the most important bond lengths and bond angles that have been computed for six zwitterionic mercury(II) complexes [HgX<sub>2</sub>Br(PPh<sub>2</sub>(CH<sub>2</sub>)<sub>2</sub>Ph<sub>2</sub>CH<sub>2</sub>C(O)C<sub>6</sub>H<sub>4</sub>Br)] (X = Cl (**1**), Br (**2**), I (**3**)) and [HgX<sub>2</sub>Br(PPh<sub>2</sub>(CH<sub>2</sub>)<sub>2</sub>Ph<sub>2</sub>CH<sub>2</sub>C(O)C<sub>6</sub>H<sub>4</sub>NO<sub>2</sub>)] (X = Cl (**4**), Br (**5**), I (**6**)). The final optimized geometries of investigated complexes (**4**-**6**) are shown in Fig. 4, and for other complexes are available in supplementary data (see Fig. 1S). The geometrical parameters for latter complexes are in generally good agreement with corresponding experimental values (see Table 7). The latter results show that the nature of the halogen atoms around metal and R group has a slight effect on the Hg-P bond length. On the other hand, the Hg-P bond length in **1** and **4** complexes (containing two chlorides) is shorter than the other computed complexes (without chloride). In comparison, our results are in good agreement with the observed experimental values in similar complexes [8].

**Table 7**

A comparison between the selected calculated bond lengths (Å) and bond angles (°) for complexes **1**-**6** and corresponding experimental values for **4** and similar complex.<sup>a</sup>

	<b>1</b>	<b>2</b>	<b>3</b>	<b>4</b>			<b>5</b>	<b>6</b>
				CEP-121G	X-ray	X-ray <sup>a</sup>		
<i>Bond lengths</i>								
Hg-P(1)	2.527	2.578	2.602	2.502	2.460	2.486	2.567	2.583
Hg-X(1) <sup>b</sup>	2.624	2.731	2.767	2.638	-	2.574	2.687	2.822
Hg-X(2) <sup>b</sup>	2.552	2.659	2.794	2.573	-	2.579	2.742	2.611
Hg-Br	2.590	2.602	2.821	2.592	-	2.522	2.606	2.756
P(1)-C(13)	1.938	1.938	1.931	1.945	1.826	1.839	1.947	1.950
C(13)-C(14)	1.553	1.554	1.556	1.542	1.518	-	1.542	1.542
C(14)-P(2)	1.897	1.899	1.904	1.896	1.806	1.816	1.897	1.897
P(2)-C(27)	1.889	1.889	1.892	1.897	1.813	1.810	1.897	1.897
C(27)-C(28)	1.534	1.533	1.531	1.534	1.515	1.511	1.534	1.534
C(28)-O(1)	1.268	1.268	1.269	1.261	1.217	1.230	1.261	1.261
<i>Bond angles</i>								
P(1)-Hg-X(1)	96.39	98.96	111.48	103.15	-	109.81	108.39	110.27
P(1)-Hg-X(2)	92.73	91.71	91.04	95.69	-	100.50	97.56	94.99
P(1)-Hg-Br	137.83	135.43	134.36	135.46	-	126.85	133.51	132.36
X(1)-Hg-Br	119.44	117.93	111.78	102.75	-	106.30	106.41	108.76
X(2)-Hg-Br	99.09	94.99	89.59	101.04	-	106.39	97.15	94.26
X(1)-Hg-X(2)	103.14	106.62	109.63	105.84	-	104.90	109.44	112.37

<sup>a</sup> Observed values for complex [HgCl<sub>2</sub>(Br)(Ph<sub>2</sub>PCH<sub>2</sub>PPh<sub>2</sub>CHC(O)Ph)] [8].

<sup>b</sup> X(1) and X(2) in **1** and **4** is Cl; in **2** and **5** is Br; in **3** and **6** is I.

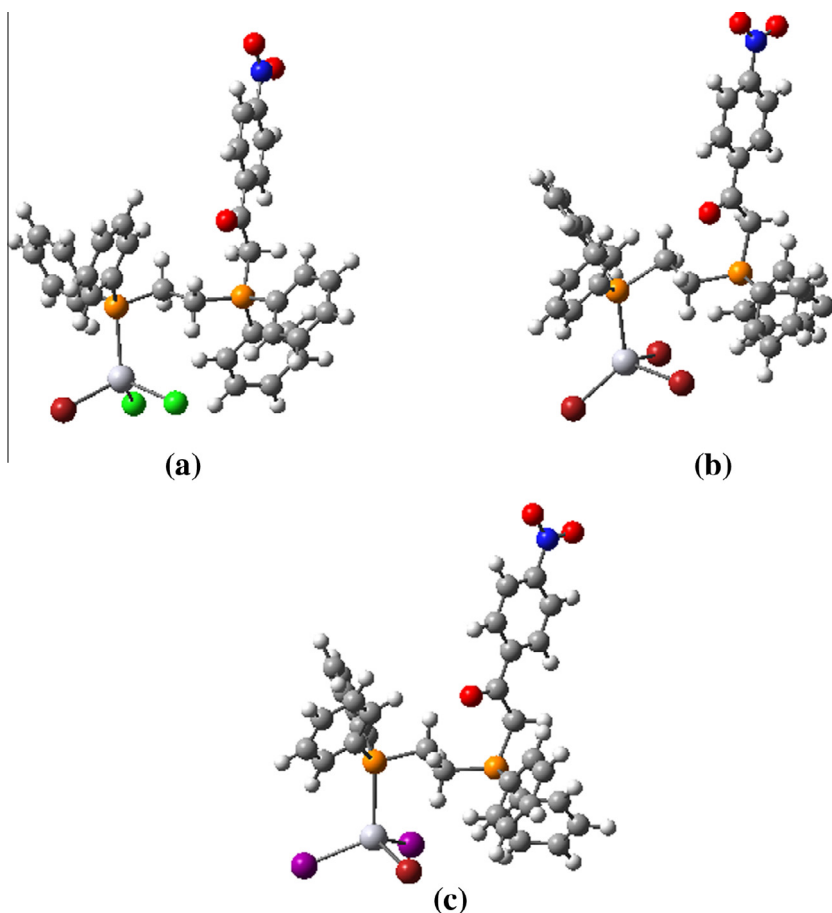


Fig. 4. The optimized geometry structures of studied complexes (a) **4**, (b) **5** and (c) **6**.

**Table 8**

The calculated thermodynamic parameters for possible reactions shown in Scheme 2 using the DFT-based B3LYP/CEP-121G method.

R	Br		NO <sub>2</sub>	
	1:1	2:1	1:1	2:1
E <sub>stb</sub>	-8.52	-5.55	-3.37	-0.017
ΔH°	-9.11	-6.14	-3.96	-0.61
ΔG°	-1.27	1.45	-3.51	7.095

E<sub>stb</sub> (kcal mol<sup>-1</sup>) is the stabilization energy of the process; ΔH° (kcal mol<sup>-1</sup>) is the enthalpy change of the process; ΔG° (kcal mol<sup>-1</sup>) is the Gibbs free energy change of the process.

We were interested that the structures of complexes **3** and **6** are determined by X-ray crystallography because of the different reported structures for these types of complexes [8,9]. However, in spite of all attempts, none of the iodine complexes have been obtained in crystalline state. Thus, the reaction between free ligands and HgI<sub>2</sub> has been investigated by DFT calculation. We are considered two possible products (1:1 and 2:1) as following scheme.

The thermodynamic parameters such as stabilization energy (E<sub>stb</sub>), Gibbs free energy changes (ΔG°), the enthalpy changes (ΔH°), and the entropy change of process (ΔS°) were calculated at B3LYP/CEP-121G level of theory for both 1:1 and 2:1 products (see Table 8). The stabilization energy indicates the formation of 1:1 product is more stable than 2:1 product. The obtained results from Table 8 indicate that the reaction of 1:1 product shown in Scheme 2 is exothermic and spontaneous, and these complexes are able to be synthesized quickly. This is in agreement with the

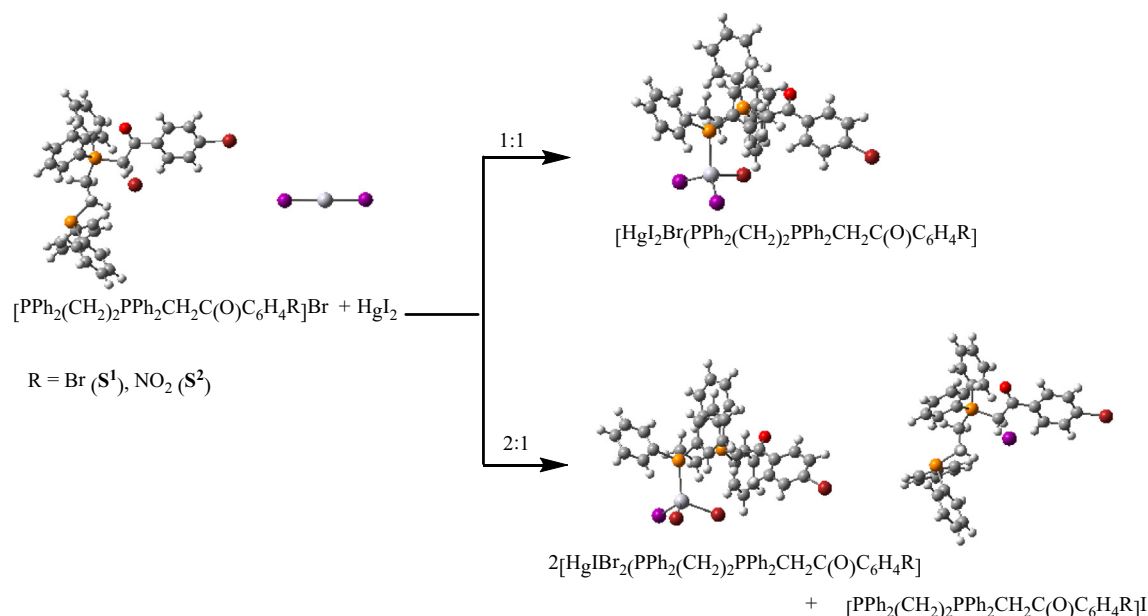
microanalysis data for the latter complexes. Hence, in spite of research down in this field [8,9], for reaction between the phosphonium salts and HgI<sub>2</sub>, our experimental and theoretical data demonstrated that the 1:1 product forms spontaneously at room temperature.

Generally, the stability of complexes is the fundamentally determined stabilization energy. From the energy point of view, the more negative stabilization energy of complexes, the more stable they are. In order to realize the stability of formed complexes, the stabilization energy (E<sub>stb</sub>) was calculated in terms of the sum of electronic energies of the structures according to the following definition as Eq. (1):

$$E_{\text{stb}} = E_{\text{complex}} - E_{\text{HgX}_2} - E_{\text{salt}} \quad (1)$$

where E<sub>complex</sub> is the energy of complex [(S<sup>1,2</sup>)MX<sub>2</sub>], E<sub>HgX<sub>2</sub></sub> is the energy of mercury(II) halides and E<sub>salt</sub> is the energy of free ligands (S<sup>1,2</sup>). The calculated stabilization energies of all complexes can be found in Table 9. According to the Eq. (1), negative and positive stabilization energies indicate that the formed complexes are stable and metastable, respectively. These results show that the complexes containing S<sup>1</sup> ligand are more stable than the complexes containing S<sup>2</sup> ligand (≈4 kcal mol<sup>-1</sup>). Along the same lines, the sequence of the calculated stabilization energies with different halogens are found as Cl > Br > I. As a result, it can be concluded that the formed complex (1) is the most stable among the others.

NBO analyses to obtain electronic properties such as the energy gap, partial charge of atoms and bond order were also investigated. The energy gap is an important parameter to characterize the chemical reactivity and kinetic stability of the molecule. A



**Scheme 2.** The possible products of reactions between ligands and  $HgI_2$ .

**Table 9**

Calculated energies for HOMO and LUMO molecular orbitals, energy gap between the HOMO and LUMO, hardness and stabilization energy ( $E_{stb}$ ) for all studied complexes.

Complex	HOMO (hartree)	LUMO (hartree)	Gap (eV)	$\eta$ (eV)	$E_{stb}$ (kcal mol <sup>-1</sup> )
1	-0.2336	-0.100	3.62	1.81	-18.85
2	-0.2291	-0.102	3.43	1.71	-12.54
3	-0.2177	-0.1046	3.07	1.53	-10.02
4	-0.2258	-0.1664	1.61	0.80	-14.65
5	-0.2207	-0.1676	1.44	0.72	-8.57
6	-0.2106	-0.1674	1.17	0.58	-4.88

molecule with a small energy gap is more polarizable, generally associated with a high chemical reactivity, low kinetic stability, and is called a soft molecule [39]. The highest occupied molecular orbital (HOMO) of one component and the lowest unoccupied molecular orbital (LUMO) are important parameters of molecular electronic structure. The hardness  $\eta$  of a molecule is defined as Eq. (1):

$$\eta = \frac{(I - A)}{2} \quad (2)$$

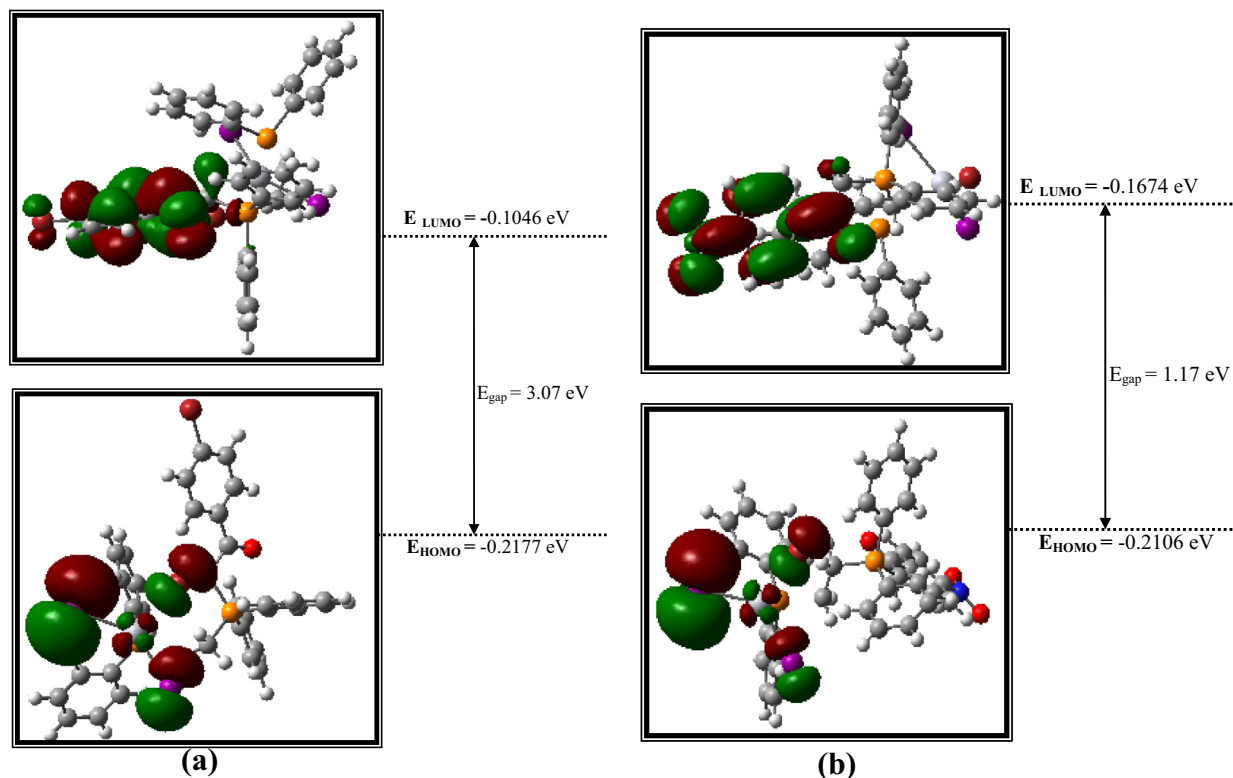


**Fig. 5.** Molecular orbital surfaces and energy level of complexes (a) 3 and (b) 6.

**Table 10**  
Wiberg bond indices (WBIs) and natural bond orbital (NBO) charges of all studied complexes.

	1	2	3	4	5	6
<i>WBIs</i>						
Hg–P(1)	0.1974	0.1757	0.1571	0.1898	0.1775	0.1671
Hg–X(1)	0.4130	0.4770	0.7218	0.4195	0.5392	0.6510
Hg–X(2)	0.5078	0.5739	0.7660	0.4818	0.6687	0.7715
Hg–Br	0.6815	0.6638	0.4025	0.6839	0.4816	0.4699
P(2)–C(27)	0.9345	0.9339	0.9347	0.9180	0.9178	0.9180
C(27)–C(28)	1.0063	1.0062	1.0054	1.0034	1.0033	1.0032
C(28)–O(1)	1.6725	1.6729	1.6725	1.7259	1.7233	1.7234
<i>NBO charges</i>						
Hg	0.7699	0.6795	0.4673	0.7614	0.6719	0.5016
X(1)	–0.6758	–0.5644	–0.4363	–0.6733	–0.5068	–0.4943
X(2)	–0.6196	–0.5075	–0.4064	–0.6418	–0.5939	–0.4040
Br	–0.5008	–0.6220	–0.6633	–0.5013	–0.6235	–0.6269
P(1)	0.7819	0.7822	0.8072	0.8214	0.8255	0.8216
P(2)	1.4317	1.4319	1.4326	1.4377	1.4375	1.4364
C(27)	–0.7161	–0.7182	–0.7110	–0.7032	–0.7015	–0.7017
C(28)	0.5730	0.57301	0.5703	0.5637	0.5635	0.5635
O(1)	–0.6086	–0.6077	–0.6088	–0.5585	–0.5605	–0.56021

X(1) and X(2) in **1** and **4** is Cl; in **2** and **5** is Br; in **3** and **6** is I.

**Table 11**  
Calculated charge transferred in all synthesized here complexes using B3LYP/CEP-121g level of theory.

Type	Charge transfer (a.u.)	Type	Charge transfer (a.u.)
S <sup>1</sup> as free ligand	0	HgX <sub>2</sub> as free ligand	0
S <sup>1</sup> in complex <b>1</b>	0.5255	HgCl <sub>2</sub> in complex <b>1</b>	–0.5255
S <sup>1</sup> in complex <b>2</b>	0.5069	HgBr <sub>2</sub> in complex <b>2</b>	–0.5069
S <sup>1</sup> in complex <b>3</b>	0.3754	HgI <sub>2</sub> in complex <b>3</b>	–0.3754
S <sup>2</sup> as free ligand	0	HgX <sub>2</sub> as free ligand	0
S <sup>2</sup> in complex <b>4</b>	0.5537	HgCl <sub>2</sub> in complex <b>4</b>	–0.5537
S <sup>2</sup> in complex <b>5</b>	0.4288	HgBr <sub>2</sub> in complex <b>5</b>	–0.4288
S <sup>2</sup> in complex <b>6</b>	0.3966	HgI <sub>2</sub> in complex <b>6</b>	–0.3966

where *I* and *A* are the ionization potential and the electron affinity of the system, respectively. Obviously, the energy gap between the HOMO and LUMO is equal to (*I* – *A*) [40,41]. Therefore, we can easily calculate the hardness of the present molecules using equation Eq. (2):

$$\eta = \frac{(E_{\text{LUMO}} - E_{\text{HOMO}})}{2} \quad (3)$$

Herein, we consider the gap energy since it is known to be an index of both kinetic stability (reactivity) and electrical conductivity. The calculated HOMO and LUMO energies, energy gap and hardness of all complexes are also summarized in Table 9. Upon going from complex **1** to **6**, the energy gap consistently decrease. It is interesting to note that the energy gap of complexes including Br group (**1–3**) are significantly higher than the complexes including NO<sub>2</sub> group (**4–6**). In this regard, for metal complexes with different halogens, the energy gap increases in this order Cl > Br > I. These results are completely consistent with the results obtained for the stabilization energy. The distribution and energy levels of the HOMO and LUMO orbitals for the studied complexes **3** and **6** are shown in Fig. 5. As can be seen, the HOMO orbital is only distributed over the metal and halogen coligands and LUMO orbital is only localized on CH<sub>2</sub>C(O)R moiety of ligand.

The natural charge of some atoms and the WBI values are listed in Table 10. Note that the total charge of the molecules is zero. The calculated NBO charge distribution indicates that the phosphorus and metal atoms always carry positive charge and the oxygen, halogen and methene carbon atoms convey negative charge. For metal complexes with different halogen atoms, the positive charge

on mercury changes in order Cl > Br > I. The effect of halogen atoms on the charge distribution parallels their electronegativities. Besides, the analysis of charge transfer between free ligands and mercury(II) halides is considered. The charge transferred between ligand and mercury(II) halides is measured as the sum of natural charges of all atoms related to the phosphonium salt and HgX<sub>2</sub>

**Table 12**  
Antibacterial activity data of free ligands and their mercury(II) complexes.

Compound	Conc. (mg/mL)	Inhibition zone (mm)			
		<i>E. coli</i> (–)	<i>P. aeruginosa</i> (–)	<i>S. aureus</i> (+)	<i>B. cereus</i> (+)
Ligand S <sup>1</sup>	5	n.a.	14	12	n.a.
	10	n.a.	15	14	n.a.
	20	n.a.	18	14	n.a.
	40	n.a.	22	21	10
Complex <b>1</b>	5	17	18	13	8
	10	18	24	13	10
	20	18	27	15	11
	40	21	30	17	14
Complex <b>2</b>	5	17	26	12	11
	10	17	28	15	12
	20	19	40	15	14
	40	21	44	19	14
Complex <b>3</b>	5	17	28	15	11
	10	18	30	15	12
	20	18	32	17	13
	40	21	32	17	15
Ligand S <sup>2</sup>	5	n.a.	9	8	n.a.
	10	n.a.	10	9	n.a.
	20	n.a.	14	11	n.a.
	40	n.a.	22	17	n.a.
Complex <b>4</b>	5	16	25	15	11
	10	17	25	16	13
	20	19	25	18	15
	40	21	29	20	17
Complex <b>5</b>	5	19	40	18	13
	10	19	40	18	15
	20	20	30	21	18
	40	23	40	26	24
Complex <b>6</b>	5	18	20	16	10
	10	18	23	16	10
	20	20	26	18	13
	40	22	28	20	18
Penicillin		12	n.a.	26	13
Gentamicin		20	20	16	21

n.a. = no activity.

obtained at the B3LYP/CEP-121 g level of theory (see Table 11). The results indicate that the significant charge transfer ( $\approx 0.45$  a.u.) from the ligands to the metal and halogen coligands is occurred.

The WBI value arises from the manipulation of the density matrix in the orthogonal natural atomic orbital basis derived through the natural population analysis [42]. The WBI expresses the sum of squares of density matrix elements ( $p_{jk}$ ) and equals twice the charge density in the atomic orbital ( $p_{jj}$ ) minus the square of the charge density, and so is mathematically defined as Eq. (3):

$$WBI = \sum_k p_{jk}^2 = 2p_{jj} - p_{jj}^2 \quad (4)$$

Table 3 shows that the WBI values of Hg–P bonds in the zwitterionic complexes are significantly slight ( $\approx 0.18$ ). On the other hand, according to NBO analyses, there is no metal–ligand bonding orbital for all investigated complexes. Therefore, the electrostatic interaction plays an important role in the interaction between the metal atom and the phosphonium–phosphine ligands. This is in accordance with the above conclusion deduced from the charge distribution.

### 3.5. Biological studies

The *in vitro* antibacterial activities of the phosphonium salts and their mercury(II) complexes have been studied along with three standard antibacterial drugs, viz, Vancomycin, Streptomycin, and Gentamycin. The microorganisms used in this work include *B. cereus* and *S. aureus* as Gram-positive bacteria and *E. coli* and *P. aeruginosa* as Gram-negative bacteria. Results of antibacterial assessments of all compounds are presented in Table 12. The data displays that the concentration of all compounds plays an important role by increasing the degree of inhibition as the concentration increases. Comparing the antibacterial activities of samples with standard drugs demonstrate that the metal complexes have remarkable inhibitory potencies against bacterial species taken in the study (see Fig. 6).

A comparative study of the growth inhibition zone values between two free ligands indicate that the activity of free ligand **S<sup>1</sup>** was higher than the activity of **S<sup>2</sup>**, and it is interesting that the latter ligands only exhibits antibacterial activity against on *P. aeruginosa* and *S. aureus*, while is not active against on *E. coli* and *B. cereus*. Thus, similar to earlier results, the activity of the ligands

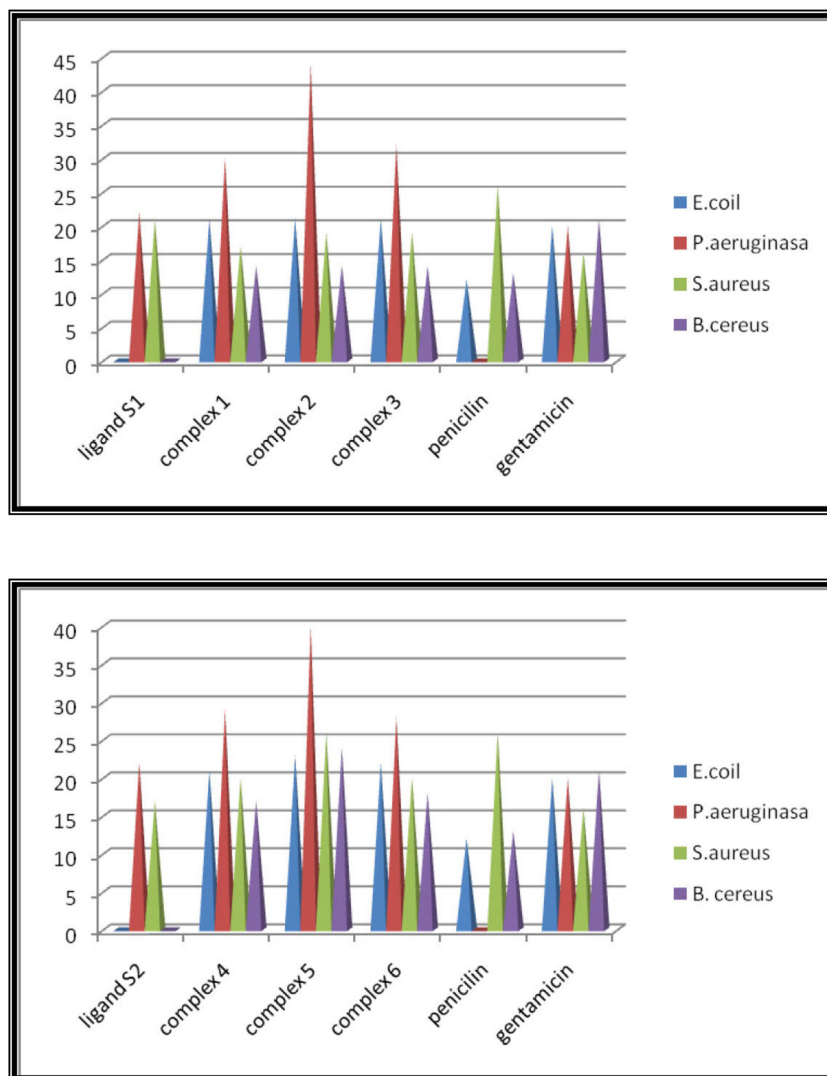


Fig. 6. Antibacterial activities of two phosphonium–phosphine salts and their mercury(II) complexes against *B. cereus* and *S. aureus* as Gram-positive bacteria and *E. coli* and *P. aeruginosa* as Gram-negative bacteria.

was slightly affected by the nature of the substituent in the *para* position of the phenyl ring of benzoyl group, and this can be explained by the lipophilicity of the ligands and their membrane permeability, a key factor in determining of their entry inside the cells [43].

On the other hand, a remarkably high activity of all complexes (1–6) was observed in comparison with the free ligands. Generally, the antibacterial activity of compounds is attributed mainly to its major components. However, today it is known that the synergistic or antagonistic effect of one compound even when it is a minor component of mixture has to be considered [44,45]. It seems that the formation of complexes may facilitate crossing of the lipid layer of the bacterial cell membrane and in this way may effect on the mechanisms of growth and development of bacteria [46,47]. Surprisingly, *P. aeruginosa* revealed high sensitivity to both groups of the studied mercury complexes, while standard drugs were found to have no activity against it. Furthermore, the halide groups coordinated to metal ions exerts a number of changes on antibacterial activity of the tested complexes. The results of antibacterial assay express that the complexes reported herein may be used for control of pathogenic bacteria.

#### 4. Conclusion

The present study describes the synthesis and characterization of six new zwitterionic complexes (1–6) with phosphonium-phosphine salts containing dppe. On the basis of the physico-chemical and spectroscopic data is clear that the phosphonium salts as ligands exhibit monodentate P-coordination to metal center, as their coordination to metal have been unequivocally confirmed by the X-ray crystal structure of complex 4. Also we have used density functional theory to analyze the electronic and molecular structure along with stability of two phosphonium salts and their mercury(II) complexes. The calculated geometries are in good agreement with available experimental values. Due to the obtained values of bonding energy and the partial atomic charges on phosphorus atoms, it can be considered that there is an interaction between bromine ion and phosphorus atom of phosphonium group in compounds **S**<sup>1</sup> and **S**<sup>2</sup>. Computed binding energies indicate that the formation of complex 1 is the most stable among the others. The results of NBO analyses show that the electrostatic interaction plays an important role in the interaction between the metal atom and the phosphonium-phosphine ligands, and the charge transfer from the ligands to the metal atom and halogen co-ligands is occurred. The remarkable change in the value of energy gap occurs upon changing the R group on benzoyl moiety. Antibacterial studies represented good inhibitory effects against both Gram-negative and -positive bacterial species, which may help to inform the design of improved antibacterial agents.

#### Acknowledgements

We are grateful to Shahid Chamran University of Ahvaz – Iran for financial support.

#### Appendix A. Supplementary data

CCDC 1027987 contains the supplementary crystallographic data for complex 4. These data can be obtained free of charge via <http://www.ccdc.cam.ac.uk/conts/retrieving.html>, or from the Cambridge Crystallographic Data Centre, 12 Union Road,

Cambridge CB2 1EZ, UK; fax: (+44) 1223-336-033; or e-mail: [deposit@ccdc.cam.ac.uk](mailto:deposit@ccdc.cam.ac.uk). Supplementary data associated with this article can be found, in the online version, at <http://dx.doi.org/10.1016/j.poly.2015.06.019>.

#### References

- [1] R. Chauvin, Eur. J. Inorg. Chem. (2000) 577.
- [2] T. Gädt, K. Eichele, L. Wesemann, Organometallics 25 (2006) 3904.
- [3] M. Stradiotto, K.D. Hesp, R.J. Lundgren, Angew. Chem., Int. Ed. 49 (2010) 494.
- [4] R.J. Lundgren, M.A. Rankin, R. McDonald, G. Schatte, M. Stradiotto, Angew. Chem., Int. Ed. 46 (2007) 4732.
- [5] M. Delferro, D. Cauzzi, R. Pattacini, M. Tegoni, C. Graiff, A. Tiripicchio, Eur. J. Inorg. Chem. (2008) 2302.
- [6] G.M. Kosolapoff, L. Maier, Organophosphorus Compounds, Wiley Interscience, New York, 1972.
- [7] J. Vicente, M.T. Chicote, M.C. Lagunas, Inorg. Chem. 36 (1997) 4938.
- [8] M.M. Ebrahim, K. Panchanatheswaran, A. Neels, H. Stoekli-Evans, Polyhedron 28 (2009) 1017.
- [9] S.J. Sabounchei, M. Panahimehr, H. Keypour, M.H. Zebarjadian, J. Mol. Struct. 1040 (2013) 184.
- [10] C. Gracia, G. Marco, R. Navarro, P. Romero, T. Soler, E.P. Urriolabeitia, Organometallics 22 (2003) 4910.
- [11] L.R. Falvello, S. Fernández, C. Larraz, R. Llusar, Rafael Navarro, E.P. Urriolabeitia, Organometallics 20 (2001) 1424.
- [12] S.A. Weicker, J.W. Dube, P.J. Ragogna, Organometallics 32 (2013) 6681.
- [13] J.W. Dube, C.L.B. Macdonald, B.D. Ellis, P.J. Ragogna, Inorg. Chem. 52 (2013) 11438.
- [14] K. Takuma, T. Takata, T. Endo, Macromolecules 26 (1993) 862.
- [15] T. Toneri, F. Sanda, T. Endo, J. Polym. Sci. Part A: Polym. Chem. 6 (1998) 1957.
- [16] T. Toneri, F. Sanda, T. Endo, Macromolecules 34 (2001) 1518.
- [17] T. Toneri, F. Sanda, T. Endo, J. Photopolym. Sci. Technol. 12 (1999) 159.
- [18] T. Toneri, K.I. Watanabe, F. Sanda, T. Endo, Macromolecules 32 (1999) 1293.
- [19] E.P. Urriolabeitia, Top. Organometall. Chem. 30 (2010) 15.
- [20] E.P. Urriolabeitia, Dalton Trans. (2008) 5673.
- [21] H. Koezuka, G. Matsubayashi, T. Tanaka, Inorg. Chem. 25 (1976) 417.
- [22] M. Kalyanasundari, K. Panchanatheswaran, W.T. Robinson, H. Wen, J. Organomet. Chem. 491 (1995) 103.
- [23] S.J. Sabounchei, H. Nemattalab, S. Salehzadeh, M. Bayat, H.R. Khavasi, H. Adams, J. Organomet. Chem. 693 (2008) 1975.
- [24] A. Spannenberg, W. Baumann, U. Rosenthal, Organometallics 19 (2000) 3991.
- [25] S.M. Sbovata, A. Tassan, G. Facchin, Inorg. Chim. Acta 361 (2008) 3177.
- [26] M.M. Ebrahim, H. Evans, K. Panchanatheswaran, Polyhedron 26 (2007) 3491.
- [27] L.R. Falvello, M.E. Margalejo, R. Navarro, E.P. Urriolabeitia, Inorg. Chim. Acta 347 (2003) 75.
- [28] A.J. Gordon, R.A. Ford, The Chemist's Companion – A Handbook of Practical Data Techniques and References, Wiley-Interscience, New York, 1972.
- [29] S.J. Sabounchei, S. Samiee, D. Nematollahi, A. Naghipour, D. Morales-Morales, Inorg. Chim. Acta 363 (2010) 3973.
- [30] S.J. Sabounchei, S. Samiee, S. Salehzadeh, M. Bayat, Z.B. Nojini, D. Morales-Morales, Inorg. Chim. Acta 363 (2010) 1254.
- [31] G.M. Sheldrick, Acta Crystallogr., Sect. A 64 (2008) 112.
- [32] O.V. Dolomanov, L.J. Bourhis, R.J. Gildea, J.A.K. Howard, H. Puschmann, J. Appl. Crystallogr. 42 (2009) 339.
- [33] (a) A.D. Becke, J. Chem. Phys. 98 (1993) 5648; (b) C. Lee, W. Yang, G. Parr, Phys. Rev. B 37 (1988) 785.
- [34] (a) T.R. Cundari, W.J. Stevens, J. Chem. Phys. 98 (1993) 5555; (b) W.J. Stevens, M. Krauss, H. Basch, P.G. Jasien, Can. J. Chem. 70 (1992) 612; (c) W.J. Stevens, H. Basch, M. Krauss, J. Chem. Phys. 81 (1984) 6026.
- [35] HYPERCHEM, Released 5.02, Hypercube Inc., Gainesville, 1997.
- [36] E.D. Glendening, A.E. Reed, J.E. Carpenter, F. Weinhold, NBO Version 3.1 TCI, University of Wisconsin, Madison, 1998.
- [37] M.J. Frisch, G.W. Trucks, H.B. Schlegel, et al., GAUSSIAN 03, Revision B.03, Gaussian Inc., Pittsburgh, PA, 2003.
- [38] A. Lledós, J.J. Carbó, E.P. Urriolabeitia, Inorg. Chem. 40 (2001) 4913.
- [39] L.R. Radovic, B. Bockrath, J. Am. Chem. Soc. 127 (2005) 5917.
- [40] R.G. Pearson, Inorg. Chem. 27 (1988) 734.
- [41] P.K. Chattaraj, A. Poddar, J. Phys. Chem. A 103 (1999) 8691.
- [42] K.B. Wiberg, Tetrahedron 24 (1968) 1083.
- [43] N.T. Abdel-Ghani, A.M. Mansour, Inorg. Chim. Acta 373 (2011) 249.
- [44] J.E. Gray, P.R. Norton, R. Alnouno, C.L. Marolda, M.A. Valvano, K. Griffiths, Biomaterials 24 (2003) 2759.
- [45] S. Burt, Int. J. Food Microb. 94 (2004) 223.
- [46] N. Fahmi, I.J. Gupta, R.V. Singh, Phosphorus Sulfur Silicon Relat. Elem. 132 (1998) 1.
- [47] M. Tumer, D. Ekinci, F. Tumer, A. Bulut, Spectrochim. Acta, Part A 67 (2007) 916.